



ALMA MATER STUDIORUM
UNIVERSITÀ DI BOLOGNA

ARCHIVIO ISTITUZIONALE DELLA RICERCA

Alma Mater Studiorum Università di Bologna Archivio istituzionale della ricerca

Tracing clinothem geometry and sediment pathways in the prograding Holocene Po Delta system through integrated core stratigraphy

This is the final peer-reviewed author's accepted manuscript (postprint) of the following publication:

Published Version:

Tracing clinothem geometry and sediment pathways in the prograding Holocene Po Delta system through integrated core stratigraphy / Amorosi A.; Bruno L.; Campo B.; Costagli B.; Dinelli E.; Hong W.; Sammartino I.; Vaiani S.C.. - In: BASIN RESEARCH. - ISSN 0950-091X. - STAMPA. - 32:2(2020), pp. 206-215. [10.1111/bre.12360]

Availability:

This version is available at: <https://hdl.handle.net/11585/804848> since: 2021-02-23

Published:

DOI: <http://doi.org/10.1111/bre.12360>

Terms of use:

Some rights reserved. The terms and conditions for the reuse of this version of the manuscript are specified in the publishing policy. For all terms of use and more information see the publisher's website.

This item was downloaded from IRIS Università di Bologna (<https://cris.unibo.it/>).
When citing, please refer to the published version.

(Article begins on next page)

This is the final peer-reviewed accepted manuscript of:

Amorosi A.; Bruno L.; Campo B.; Costagli B.; Dinelli E.; Hong W.; Sammartino I.; Vaiani S.C.: *Tracing clinothem geometry and sediment pathways in the prograding Holocene Po Delta system through integrated core stratigraphy*

BASIN RESEARCH VOL. 32 ISSN: 0950-091X

DOI: 10.1111/bre.12360

The final published version is available online at:

<https://dx.doi.org/10.1111/bre.12360>

Terms of use:

Some rights reserved. The terms and conditions for the reuse of this version of the manuscript are specified in the publishing policy. For all terms of use and more information see the publisher's website.

This item was downloaded from IRIS Università di Bologna (<https://cris.unibo.it/>)

When citing, please refer to the published version.

Alessandro Amorosi¹, Luigi Bruno², Bruno Campo¹, Bianca Costagli¹, Enrico Dinelli¹, Irene Sammartino³ and Stefano Claudio Vaiani¹

Tracing clinothem geometry and sediment pathways in the prograding Holocene Po Delta system through integrated core stratigraphy

¹Department of Biological, Geological and Environmental Sciences, University of Bologna, Italy

²Department of Chemical and Geological Sciences, University of Modena and Reggio Emilia, Italy

³Geologic Consultant, Bologna, Italy

Abstract

Though clinothem geometry represents a key control on fluid flow in reservoir modeling, tracing clinothem boundaries accurately is commonly limited by the lack of sufficiently precise outcrop or subsurface data. This study shows that in basin systems with strongly heterogeneous compositional signatures, the combination of bulk-sediment geochemistry and benthic foraminiferal distribution can help identify clinothem architecture and generate realistic models of 3D deltaic upbuilding and evolution.

Middle-late Holocene deposits in the Po Delta area form an aggradational to progradational parasequence set that reveals the complex superposition of W-E delta progradation, S-directed longshore currents (from Alpine entry points) and Apennine rivers supply. Unique catchment lithologies (ophiolite rocks and dolostones) were used to delineate basin-wide geochemical markers of sediment provenance (Cr and Mg) and to assess clear detrital signatures. The geochemical characterization of cored intervals across different components of the sediment routing system enabled a direct linkage between clinothem growth, transport pathways and provenance mixing to

1
2
3 be established. On the other hand, abrupt microfaunal variations at clinothem boundaries were
4
5 observed to reflect the paleoenvironmental response to sharp changes in sediment flux and fluvial
6
7 influence.
8
9

10 This study documents the ability of an integrated geochemical and paleoecological approach to
11
12 delineate the different sources that effectively contributed to coastal progradation and to outline the
13
14 lithologically cryptic geometries of clinothems that using conventional sedimentological methods it
15
16 would be virtually impossible to restore.
17
18
19
20
21
22

23 **Introduction**

24
25
26
27
28 Prograding coastal and deltaic depositional systems are commonly examined across their
29
30 downdip components, which afford the observation of clinofolds, stratal terminations and stacking
31
32 patterns (Catuneanu et al., 2019). In contrast, scarce attention is generally paid to their development
33
34 parallel to depositional strike. Clinothems are key sedimentary elements of prograding systems that
35
36 are typically bounded by hiatal surfaces. Clinothem boundaries mark abrupt shifts in depositional
37
38 systems configuration and sediment dispersal pathways that might impact significantly oil
39
40 exploration and production. Changes in outbuilding directions within sets of clinothems, in
41
42 particular, are likely to generate heterogeneities that represent potential barriers to fluid flow (Enge
43
44 et al., 2010).
45
46
47
48

49 In subsurface studies, at the resolution of data commonly available, the geometry of individual
50
51 clinothems can hardly be assessed on a sub-seismic scale. This is increasingly evident in mudstone-
52
53 dominated systems (Bohacs et al., 2014; Lazar et al., 2015; Birgenheier et al., 2017; Pellegrini et al.,
54
55 2017; 2018), where the presence of subtle heterogeneities within seemingly homogeneous sediment
56
57 bodies cannot be deciphered based on physical sedimentary structures alone.
58
59
60

1
2
3 Sequence-stratigraphic models assume that nearshore strata have relatively consistent and
4 laterally persistent stacking at the systems tract scale (Madof et al., 2016). However, a significant
5 3D variability of the stratigraphic architecture commonly develops in response to variations in
6 accommodation and sedimentation across a sedimentary basin (Olariu and Steel, 2009). In along-
7 strike direction, the autogenic shift of distributary channels or delta lobes may affect the pattern of
8 sediment distribution. Furthermore, rates of accommodation and sedimentation may change
9 significantly at any particular location within a basin, resulting in highly diachronous sedimentary
10 units (Catuneanu et al., 2019).
11
12
13
14
15
16
17
18
19
20

21 The middle-late Holocene highstand succession of the Po Plain, in northern Italy, is a 30 m-
22 thick, mud-prone depositional system that records a complex pattern of coastal progradation and
23 delta upbuilding. The stepped progradation of the coastal plain includes a set of five millennial-
24 scale parasequences that have been well portrayed by depositional dip-oriented (SW-NE) cross-
25 sections (Amorosi et al., 2017). Recent dynamics of deltaic progradation have been outlined in
26 detail by Correggiari et al. (2005a). Since the Bronze Age, the Po Delta occupied a broad stretch of
27 the Adriatic coastal system, nourishing cusped and arcuate (wave-dominated) deltas. After 2,000
28 ky BP, changes in sediment discharge and the evolution of the Po Delta took place under
29 considerable anthropogenic influence (Maselli and Trincardi, 2013).
30
31
32
33
34
35
36
37
38
39
40
41

42 Clinostem stacking patterns transversal to transport direction have been portrayed accurately
43 from the adjacent Adriatic Sea through high-resolution seismic stratigraphy. Individual prodelta
44 lobes overlap laterally and can be traced along-strike as identifiable seismic-stratigraphic units over
45 relatively short (10-20 km) distances (Correggiari et al., 2005b). Along the mud-dominated Adriatic
46 coastline, inner-shelf mud belts are typically elongated downdrift of the Po River mouth, reflecting
47 prevailing sediment dispersal to the south (Cattaneo et al., 2003). Based on seismic-stratigraphic
48 studies, Cattaneo et al. (2003) documented that individual prodelta lobes emanating from the
49 southward oriented delta outlets are more easily preserved compared to those advancing
50 episodically to the NE. When a newly activated lobe is located updrift (north), the abandoned lobe
51
52
53
54
55
56
57
58
59
60

1
2
3 is sheltered by the new one. In contrast, when the retreating lobe is updrift, it is partly cannibalized
4
5 and transported downdrift to the new active lobe (Correggiari et al., 2005b).
6

7
8 The aim of this study, which is focused on the high-resolution sequence stratigraphy of the
9
10 prograding, middle-late Holocene Po Delta system, is to examine the potential of an integrated
11
12 geochemical and paleoecological approach to decipher clinothem boundaries within lithologically
13
14 homogeneous, mud-prone successions. Specific objective is to document the along-strike variability
15
16 of sediment composition and foraminiferal distribution as a function of the natural complexity and
17
18 interplay of fluvial dynamics and delta evolution, which may have profound impact on reservoir
19
20 heterogeneity.
21
22
23
24
25
26
27

28 **Holocene stratigraphy**

29
30
31
32

33 The Po River Basin is a foreland basin system bounded by two mountain chains: the Alps to the
34
35 north and the Apennines to the south (Fig. 1A). The Po River watershed is generated by the
36
37 catchments of tens of tributaries extending from the Western Alps to the Adriatic Sea. The Po River
38
39 is the longest river in Italy, and flows from west to east for 652 km.
40
41

42 Holocene deposits in the Po coastal plain form a typical transgressive-regressive sedimentary
43
44 wedge made up of coastal to shallow-marine facies assemblages that are vertically stacked onto
45
46 Pleistocene alluvial deposits and that extend both updip and downdip into the fully continental and
47
48 fully marine settings. Transgressive facies architecture reflects a dominant role of eustasy on
49
50 sequence development (Amorosi et al., 2017). Highstand deposits, instead, denote a dominantly
51
52 autogenic control. These latter are genetically related to the rapidly deposited mud wedge that
53
54 accumulated on the shelf for 600 km along the Adriatic coast of Italy (Trincardi et al., 1996;
55
56 Cattaneo et al., 2003; Amorosi et al., 2016).
57
58
59
60

1
2
3 Major architectural components of the Holocene succession are sediment packages developed on
4
5 millennial timescales and framed by flooding surfaces, i.e. surfaces of chronostratigraphic
6
7 significance (parasequences 1-8 in Amorosi et al., 2017). In along-strike direction, beneath the
8
9 modern shoreline, the Holocene transgressive-regressive cycle translates into a muddy
10
11 (offshore/prodelta) unit sandwiched between laterally continuous, transgressive barrier sands below
12
13 and highstand beach-ridge/delta front units above (Campo et al., 2017 - Fig. 1B).

14
15
16
17 The switch from continental to early Holocene, estuarine depositional systems (Bruno et al.,
18
19 2017) is documented by the retrogradational stacking of thin parasequences 1-3 (Amorosi et al.,
20
21 2017). Above a condensed offshore succession, five middle-late Holocene parasequences (4-8 in
22
23 Fig. 1B) stack and shingle to form, instead, a thick and complex, aggradational to progradational
24
25 highstand systems tract (HST) that preserves evidence for deltaic and coastal progradation, with
26
27 thick prodelta clay packages overlain by sand-prone, delta front facies. Within the HST, fossil
28
29 assemblages depict an upward trend from wave-influenced (lower HST) to river-dominated (upper
30
31 HST) coastal systems (Amorosi et al., 2017).

32
33
34
35 Highstand clinothems form shallowing-upward packages that are typically represented by
36
37 thickening-upward trends in sand layers and by general coarsening-upward patterns (parasequences
38
39 in Fig. 1B). Heterolithic facies typically develop between prodelta clays and extensive sheet sands
40
41 made up of delta front deposits (Bhattacharya and Giosan, 2003). Clinothem boundaries are locally
42
43 characterized by the sharp decrease in the sand/mud ratio, which reflects a lateral shift in associated
44
45 environments. In most cases, however, clinothem boundaries occur at mud-on-mud or sand-on-sand
46
47 contacts (Fig. 1B). Assessing their potential geometry from core data, thus, relies exclusively on the
48
49 interpolation of radiometric data (Amorosi et al., 2017).

50 51 52 53 54 55 56 57 58 **Methods** 59 60

1
2
3 A total of 166 core samples were analyzed for bulk-sediment geochemistry. Samples were
4 collected at depths < 30 m from 12 cores (Fig. 1B): P13N, P14N, P10N, P8N, P4N, CB, and 205-
5 S10 (Greggio et al., 2018), core 187S1 (Amorosi et al., 2007), Barr (Core1 in Amorosi et al., 2008),
6 EM7, EM12, and 187S3 (this study). The dataset includes 51 additional modern river sediment
7 samples that were used as reference samples for the geochemical characterization of source areas
8 (Fig. 2). With the aim of making geochemical data from modern river sediments comparable with
9 the variety of lithofacies assemblages identified in cores, sampling covered a broad grain-size
10 spectrum, from coarse sand to clay. Recent to sub-recent river sediments were collected from
11 subaqueous channel beds, exposed bars, and overbank fines.
12
13
14
15
16
17
18
19
20
21
22

23
24 Samples were analyzed at Bologna University laboratories for 10 major element oxides, the loss
25 on ignition (LOI) and 21 trace elements. LOI, evaluated after overnight heating at 950°C (LOI₉₅₀),
26 represents a measure of volatile substances (weight %, wt%), including pore water, inorganic
27 carbon and organic matter. The estimated precision and accuracy for trace-element determinations
28 was 5%, except for elements with low concentrations (< 10 ppm), for which the accuracy was lower
29 (10%).
30
31
32
33
34
35
36

37
38 A review of micropaleontological data from cores 187S1, 205S9, 205S10, 223S3 and Barr (e.g.
39 Campo et al., 2017; Barbieri et al., 2017), with a special emphasis on benthic foraminiferal
40 assemblages from core 187S7, was carried out to refine facies interpretation and, specifically, to
41 characterize parasequence boundaries within muddy intervals.
42
43
44
45
46
47
48

49 **Geochemical tracers of sediment provenance**

50
51
52
53

54 Owing to its situation in a complex tectonic setting, the Po Basin is supplied by a variety of
55 sediment sources that display strongly heterogeneous compositional signatures. Mafic and
56 ultramafic rocks crop out extensively in the western Alps and at the northwestern tip of the
57 Apennines, and represent exclusive catchment lithologies that were adopted to delineate basin-wide
58
59
60

1
2
3 markers of sediment provenance. These ophiolite successions consist primarily of peridotite,
4
5 gabbro, basalt and ophiolitic breccia, and deliver large volumes of Cr-rich (and Ni-rich) detritus to
6
7 the alluvial and coastal systems (Amorosi et al., 2002; Curzi et al., 2006; Amorosi and Sammartino,
8
9 2018; Greggio et al., 2018).

11
12 Thick dolostone and limestone successions are largely exposed in the Eastern (and Central) Alps,
13
14 where they make a substantial portion of Triassic platforms and build-ups. Therefore, major
15
16 elements, such as Mg and Ca (and their oxides MgO and CaO), can be used to discriminate these
17
18 source areas. Calibration with mineralogical data (Marchesini et al., 2000) has shown that Mg
19
20 enrichments in modern coastal deposits reflect erosion and transport of detrital dolomite from the
21
22 North Adriatic river catchments, which acted as sources of particular detritus to the Po coastal plain
23
24 (Amorosi et al., 2002; 2007; Curzi et al., 2006; Amorosi and Sammartino, 2018; Greggio et al.,
25
26 2018).

27
28
29
30
31 As absolute Cr, Ni, Mg and Ca concentrations also reflect hydraulic sorting and can be affected
32
33 by changes in grain size, normalization of geochemical data using one element as grain size proxy
34
35 is necessary to compensate for mineralogical and granular variability of metal concentrations.
36
37 Al_2O_3 , which is routinely used as an efficient normalization factor, proved very effective in
38
39 reducing the grain size effect and to differentiate sediment sources with distinct parent-rock
40
41 compositions (Fig. 2).

42
43
44
45 Plots of modern river samples from three different catchments (Po River, Apennines,
46
47 Central/Eastern Alps) display poor overlap in composition, and distinctive geochemical signatures
48
49 can be observed across all grain-size grades (Fig. 2). The geochemical composition of modern
50
51 stream sediments, thus, delineates primary end-members and strongly constrains provenance
52
53 inferences from Holocene deposits (Fig. 2). River sediment from the Po River invariably exhibits
54
55 high $\text{Cr}/\text{Al}_2\text{O}_3$ levels (> 12) and is associated with relatively low $\text{MgO}/\text{Al}_2\text{O}_3$ values. On the other
56
57 hand, samples from modern Alpine rivers plot considerably off this general trend, revealing a
58
59 distinctive geochemical facies with significantly higher $\text{MgO}/\text{Al}_2\text{O}_3$ values (> 0.35) that can be
60

1
2
3 readily differentiated from modern Po River samples. Modern Apennine river sediment is, instead,
4
5 typified by comparatively lower $\text{Cr}/\text{Al}_2\text{O}_3$ (< 12) and $\text{MgO}/\text{Al}_2\text{O}_3$ (< 0.4) values.
6
7

8 Compositional features of fluvial end-members were adopted to trace detrital signatures of
9
10 Holocene cored samples across along-strike segments of the sediment dispersal system (Fig. 3).
11
12 Chemostratigraphic correlations, in particular, were employed to trace provenance shifts across
13
14 lithologically uniform prodelta muds. As an example, a cut-off value of the $\text{MgO}/\text{Al}_2\text{O}_3$ ratio
15
16 targeted around 0.35 (Fig. 2) represents an effective tool for the discrimination on vertical profiles
17
18 between the Po River sediment source and dolostone-derived detritus from the Central/Eastern
19
20 Alpine rivers (Fig. 3): relatively high $\text{MgO}/\text{Al}_2\text{O}_3$ values denote sediment supplied, in part at least,
21
22 by Alpine sources and are interpreted to reflect a mixed signature of chiefly Po-derived sediment,
23
24 with a considerable supply from Eastern Alps sources. The abrupt upward decrease in the
25
26 $\text{MgO}/\text{Al}_2\text{O}_3$ ratio (Fig. 3), which is paralleled by a remarkable increase in $\text{Cr}/\text{Al}_2\text{O}_3$ values, has
27
28 stratigraphic significance and is inferred to reflect primarily the shift in sediment provenance from a
29
30 wave-influenced coastal environment, where S-directed longshore dispersal was an important
31
32 transport mechanism, to a fluvial-dominated, deltaic system, fed almost uniquely by the Po River.
33
34
35
36
37
38
39

40 **Foraminiferal distribution as a key to clinothem boundary identification**

41
42
43

44 In prograding deltaic successions characterized by fast, relatively continuous sedimentation,
45
46 clinothem boundaries are represented by hiatal stratigraphic surfaces of short duration and small
47
48 areal extent. As these surfaces commonly occur within relatively homogeneous lithosomes,
49
50 clinothem geometries may locally have poor physical expression. In such instances, based on
51
52 comparison with the modern Po Delta area, foraminiferal distribution can be used to delineate
53
54 clinothem boundaries that are independent of lithology.
55
56
57

58 Modern deltaic sediments are typified by low-diversity benthic assemblages indicative of highly-
59
60 stressed and unstable environments (Jorissen, 1988). Notably, high concentrations ($> 40\%$) of

1
2
3 *Ammonia tepida* and *Ammonia parkinsoniana* have been observed to reflect remarkable sediment
4 discharge related to flood events, in relatively shallow waters (< 20 m depth), in front of modern Po
5 river mouths (Barbieri et al., 2017). In contrast, relatively high amounts of *Aubignyna perlucida*,
6 *Criboelphidium granosum* and *Nonionella turgida* (ca 20% considered together) are typically
7 abundant far from river outlets. In distal prodelta environments, these taxa are commonly associated
8 with inner shelf species, such as *Textularia* spp. and miliolids (e.g. Campo et al., 2017, Barbieri et
9 al., 2017).

10
11
12
13
14
15
16
17
18
19
20
21
22
23
24
25
26
27
28
29
30
31
32
33
34
35
36
37
38
39
40
41
42
43
44
45
46
47
48
49
50
51
52
53
54
55
56
57
58
59
60
The possible use of paleocologic criteria for the delineation of clinothem boundaries is exemplified by the vertical distribution of benthic foraminifers in core 187-S7 (Fig. 4 - see Barbieri et al., 2017, for details). At this location, the middle-late Holocene HST consists almost entirely of mud deposits (Fig. 1B), which makes stratigraphic correlations and parasequence boundary identification very difficult. Paleoenvironmental changes in this homogeneous muddy interval can be tracked using changes in benthic foraminiferal distribution as indicators of proximity to/distance from the river mouth. Notably, the upward increase in *A. tepida* and *A. parkinsoniana* is taken as an indication of upward shoaling, and hence, it is interpreted to reflect delta lobe progradation (Fig. 4). This trend is predictably paralleled by the decrease of subordinate species, such as *A. perlucida*, *C. granosum*, and *N. turgida*. Localized, sharp declines in the dominant species (*A. tepida* and *A. parkinsoniana*) concurrent with the occurrence of inner shelf species are, instead, indicative of lower riverine influence and sudden drops in fluvial discharge, likely related to distributary channel avulsion and delta lobe switching (Fig. 4).

51 **Insight into delta evolution from the geochemical and paleoecological record**

52
53
54
55
56
57
58
59
60
The integration and mutual calibration of two independent data sets (bulk-sediment geochemistry and benthic foraminiferal analysis) can be used to generate a model of deltaic and coastal evolution in the Po coastal plain, over the last ca. 6 cal ky BP (parasequences 4 to 8 in Fig. 5). Cyclic

1
2
3 depositional patterns are interpreted as driven by autogenic processes (Amorosi et al., 2017), and
4
5 compensation stacking of mouth bars is proposed as the origin of these packages (Enge et al.,
6
7 2010).
8
9

10 The geochemical characterization of the HST reflects remarkable along-strike variability of
11
12 dispersal patterns. As a whole, provenance signals proved to be poorly affected by lithologic
13
14 variation, and are consistent on a depositional system scale, being detectable across both delta front
15
16 sands and prodelta muds. In general, the prograding Po delta acted as the major source of sediment
17
18 to the Adriatic coastal system. However, the proportional contribution of Alpine sources to the
19
20 coastal region varied continuously as the Po River mouths approached or moved away from the
21
22 study area. Generally high MgO/Al_2O_3 levels and concurrent low Cr/Al_2O_3 values along the
23
24 relatively flat, distal segments of older clinothems (parasequences 4-5 along profile AA' in Fig. 5)
25
26 suggest that between about 6.0-2.8 cal ky BP Alpine, dolostone-rich river catchments represented a
27
28 key sediment delivery system for wave-influenced deltas in the Adriatic area via the south-directed
29
30 longshore drift. During this phase, the Adriatic coastal system experienced weak progradation, and
31
32 E-dipping clinothems fed by the Po River (parasequences 4 and 5 along transversal profiles in Fig.
33
34 5) were restricted to proximal locations.
35
36
37
38

39 Parasequence 6 documents contrasting geochemical signatures in the southern and northern
40
41 regions along profile AA' (Figs. 3 and 5). Comparatively low MgO/Al_2O_3 values and high Cr/Al_2O_3
42
43 levels south of transect DD' exhibit strong affinity with modern Po River sediment composition
44
45 (Fig. 3) and arguably reflect Po Delta initiation in that area. The southern branch of the Po River
46
47 (*Po di Spina*) likely represented the fluvial feeder system of these southern clinothems (Correggiari
48
49 et al., 2005a), as documented by the closer affinity of cored samples with the Cr-rich compositions
50
51 typical of sediment derived from the Po River catchment (Fig. 2). At more northward locations,
52
53 geochemical data from both sands and muds suggest mixed, fluvial-wave dispersal, with a dominant
54
55 Alpine contribution and a subordinate, Po supplied component (Figs. 3 and 5).
56
57
58
59
60

1
2
3 Given the counter-clockwise oceanic circulation pattern of the Northern Adriatic Sea (Cattaneo
4 et al., 2003), it is likely that sand of Alpine provenance was transported by S-directed, longshore
5 currents, whereas mud was probably resuspended by storms and wave action above storm wave
6 base, and advected alongshore by geostrophic currents for long distances along the paleoshelf.
7 During this period, the (river-dominated) *Po di Spina* delta system was more protrusive than its
8 wave-dominated counterparts in the north, and likely represented a barrier to southerly directed
9 longshore transport (Fig. 5).

10
11
12 The prominent shift in sediment composition from Alpine feeding sources to a dominant Po
13 River contribution (Fig. 3), which marks the boundary between parasequences 6 and 7 (Fig. 5),
14 reflects the historical activation of the *Po di Volano* branch, north of the *Po di Primaro* river mouth,
15 and denotes the ultimate replacement of S-directed (Alpine) sediment supply with sediment from
16 prograding Po delta lobes. More in general, this change in bulk-sediment composition reflects the
17 switch from wave-dominated (Cr-poor and Mg-rich) to river-dominated (Cr-rich and Mg-poor)
18 depositional systems, which occurred in response to delta upbuilding. From the Middle Ages
19 onwards, sediment composition of parasequences 7 and 8 (Fig. 1B) largely reflects deltaic
20 sedimentation supplied from the Po River, whereas southern regions denote a geochemical
21 signature from Apennine entry points (Fig. 5).

22
23
24 The mid 12th century (ca. 800 yr BP) natural avulsion (*Rotta di Ficarolo*) that shifted the main
25 trunk of the Po River towards its present position (Correggiari et al., 2005a) is marked by the
26 boundary between parasequences 7 and 8 (*Po di Goro* delta system in Fig. 5). This stratigraphic
27 surface has no geochemical expression, as it separates two delta lobes of different age, but similar
28 composition. In this case, shifts in river mouth and delta lobe abandonment were detected by abrupt
29 shifts in benthic foraminiferal distribution (Fig. 4).

30
31
32 The combined geochemical and paleoecologic approach adopted in this work is highly
33 reproducible in the ancient record and has the potential to reliably constrain sediment-budget
34 modeling in sedimentary basins with multiple entry points. It is best suited to subsurface
35
36
37
38
39
40
41
42
43
44
45
46
47
48
49
50
51
52
53
54
55
56
57
58
59
60

1
2
3 stratigraphic analysis, where it may enable new insights into the interpretation of clinothem stacking
4 patterns, avoiding arbitrary or unrealistic correlation of sparse core data. In hydrocarbon
5 exploration, this technique may guide the delineation of sediment bodies with distinct sediment
6 composition, predictable lateral extent and well-defined petrophysical properties.
7
8
9
10
11
12
13
14
15
16

17 **Conclusions**

18
19
20
21 Prograding clinothem sets may have a poor lithologic expression, especially in mud-prone delta
22 systems, and they can be easily missed on a sub-seismic scale. This study shows that sharp changes
23 in parent-rock composition and benthic foraminifera communities can provide the key criteria for
24 deciphering subtle heterogeneities and cryptic stratigraphic patterns at the core scale, allowing for
25 accurate control of three-dimensional stratigraphic complexity.
26
27
28
29
30
31
32

33 The chemostratigraphic analysis of the middle-late Holocene succession from the Po Basin
34 documents that methods for source discrimination based on bulk-sediment geochemistry, when
35 calibrated with mineralogical data in a highly constrained sequence-stratigraphic framework, can be
36 effective for a sound assessment of the routing system and can ultimately allow quantification of
37 sediment fluxes below the resolution of seismic data. In multi-sourced sediment-supply systems,
38 unique source rocks control the spatial variation of elemental tracers at the basin scale and carry
39 distinct geochemical fingerprints that may propagate to deltaic, coastal, and shallow marine
40 depositional systems, and that can be applied with equal success to sand, silt and clay fractions.
41 Major and trace element composition of cored samples was matched against geochemical features
42 of samples from the modern river network. Notably, changes in sediment dispersal pathways were
43 detected using key element ratios, such as $\text{Cr}/\text{Al}_2\text{O}_3$ and $\text{MgO}/\text{Al}_2\text{O}_3$, where the former is a proxy
44 for the mafic/ultramafic contribution, and the latter is discriminant for dolostone-derived detritus.
45
46
47
48
49
50
51
52
53
54
55
56
57
58
59
60

1
2
3 Through combined sedimentologic, paleontologic and geochemical investigations,
4
5 chronologically constrained by a wealth of radiocarbon dates, this study demonstrates that tracing
6
7 clinoformal geometries within stratigraphic units characterized by relatively continuous sediment
8
9 accumulation is possible even away from seismic imaging. Changes in sediment composition and/or
10
11 foraminiferal distribution, rather than grain size, are the primary defining features of clinothem
12
13 boundaries and are diagnostic to the identification of these surfaces. This approach can be applied
14
15 successfully to analogous Quaternary subsurface successions and also has a strong potential in
16
17 outcrop studies, where clinothem boundaries may have no obvious lithologic expression and
18
19 dipping geometries can be too low to be traced confidently.
20
21
22

23
24 At the parasequence (millennial) scale of investigation illustrated in this paper, this
25
26 ‘unconventional’ approach provides insight into the potential complexities of sediment fluxes that
27
28 can be useful for guiding interpretation of prograding deltaic and coastal successions in the ancient
29
30 record. In particular, it can be used to constrain, correlate and map sediment packages that may
31
32 otherwise be difficult to separate and quantify, and can be applied to developing shale hydrocarbon
33
34 resources in mudstone-dominated systems.
35
36
37
38
39
40
41
42
43
44
45
46
47
48
49
50
51
52
53
54
55
56
57
58
59
60

Figure captions

Fig. 1. A: Regional setting and location of the study area. B: Strike-oriented fence diagram, showing the three-dimensional stratigraphic architecture of the Holocene succession of the Po Basin, and its subdivision into parasequences (based on Amorosi et al., 2017).

Fig. 2. Scatterplots of MgO/Al_2O_3 versus Cr/Al_2O_3 , showing contrasting sediment composition of modern Po River, and selected Alpine and Apennine rivers.

Fig. 3. Vertical profiles of MgO/Al_2O_3 in along-strike direction (Fig. 1B), showing the abrupt provenance shift from predominantly Alpine sediment sources to the Po River sediment supply (see Fig. 5). The cut-off value at 0.35 used for the differentiation of Alpine and Po sediment sources is consistent with modern river sediment composition (Fig. 2). Relatively high MgO/Al_2O_3 values in the uppermost two samples from core 187-S3 are associated with extremely high Cr/Al_2O_3 levels, and thus reflect a Po River source.

Fig. 4. Abrupt change in foraminiferal assemblage at the boundary (PB) between *Po di Volano* and *Po di Goro* delta lobes (= boundary between parasequences 7 and 8 in core 187-S7 - Figs. 1B and 5). Sample at 22.10 m depth is dominated by *Ammonia tepida* (At) and *A. parkinsoniana* (Apa), whereas sample at 21.60 m depth, just above PB, shows a significantly more diversified assemblage, involving *Aubignyna perlucida* (Ape), *Nonionella turgida* (Nt), *Textularia agglutinans* (Ta), *Criboelphidium granosum* (Cg), and miliolids (Al: *Adelosina longirostra*; Qs: *Quinqueloculina seminulum*; Ms: *Miliolinella subrotunda*; Tr: *Triloculina rotunda*; Tt: *T. trigonula*). Scale bar: 200 μ m.

Fig. 5. Strike-oriented fence diagram of Figure 1B, which affords the visualization of the sediment-transport system as a function of parasequence architecture and of its evolution through time. The red asterisk shows the stratigraphic location of Figure 4. LST: lowstand systems tract, TST: transgressive systems tract, HST: highstand systems tract.

References

AMOROSI A., SAMMARTINO I., 2018. Shifts in sediment provenance across a hierarchy of bounding surfaces: A sequence-stratigraphic perspective from bulk-sediment geochemistry. *Sediment. Geol.*, **375**, 145–156.

AMOROSI, A., CENTINEO, M.C., DINELLI, E., LUCCHINI, F., TATEO, F., 2002. Geochemical and mineralogical variations as indicators of provenance changes in Late Quaternary deposits of SE Po Plain. *Sediment. Geol.*, **151**, 273–292.

AMOROSI, A., COLALONGO, M.L., DINELLI, E., LUCCHINI, F., VAIANI, S.C. 2007. Cyclic variations in sediment provenance from Late Pleistocene deposits of Eastern Po Plain, Italy. In Arribas J., Critelli S., Johnsson M.J. (Eds.) *Sedimentary Provenance and Petrogenesis: Perspectives from Petrography and Geochemistry*. Geol. Soc. America – Spec. Paper **420**, 13–24.

AMOROSI, A., DINELLI, E., ROSSI, V., VAIANI, S.C., SACCHETTO M., 2008. Late Quaternary palaeoenvironmental evolution of the Adriatic coastal plain and the onset of Po River Delta. *Palaeogeogr., Palaeoclimatol., Palaeoecol.*, **268**, 80–90.

AMOROSI, A., MASELLI, V., TRINCARDI, F., 2016. Onshore to offshore anatomy of a late Quaternary source-to-sink system (Po Plain–Adriatic Sea, Italy). *Earth-Sci. Rev.*, **153**, 212–237.

AMOROSI, A., BRUNO, L., CAMPO, B., MORELLI, A., ROSSI, V., SCARPONI, D., HONG, W., BOHACS, K.M. & DREXLER, T.M., 2017. Global sea-level control on local parasequence architecture from the Holocene record of the Po Plain, Italy. *Mar. Petrol. Geol.*, **87**, 99–111.

- 1
2
3 BARBIERI G., AMOROSI A., VAIANI, S.C., 2017. Benthic foraminifera as a key to delta
4 evolution: A case study from the late Holocene succession of the Po River Delta.
5
6
7
8 Micropaleontology, **63**, 27–41.
9
10
11
12 BHATTACHARYA, J.P., GIOSAN, L., 2003. Wave-influenced deltas: Geomorphological
13 implications for facies reconstruction. *Sedimentology*, 50, 187–210.
14
15
16
17
18
19 BIRGENHEIER, L.P., HORTON, B., MCCAULEY, A.D., JOHNSON, C.L., KENNEDY, A.,
20
21 2017. A depositional model for offshore deposits of the lower Blue Gate Member, Mancos Shale,
22
23 Uinta Basin, Utah, USA. *Sedimentology*, **64**, 1402–1438.
24
25
26
27
28 BOHACS, K.M., LAZAR, O.R., DEMKO, T.M., 2014. Parasequence types in shelfal mudstone
29 strata—Quantitative observations of lithofacies and stacking patterns, and conceptual link to
30
31 modern depositional regimes. *Geology*, **42**, 131–134.
32
33
34
35
36
37 BRUNO, L., BOHACS, K.M., CAMPO, B., DREXLER, T.M., ROSSI, V., SAMMARTINO, I.,
38
39 SCARPONI, D., HONG, W., AMOROSI, A., 2017. Early Holocene transgressive palaeogeography
40
41 in the Po coastal plain (northern Italy). *Sedimentology*, 64, 1792–1816.
42
43
44
45
46
47 CAMPO, B., AMOROSI, A. & VAIANI, S.C., 2017. Sequence stratigraphy and late Quaternary
48 paleoenvironmental evolution of the Northern Adriatic coastal plain (Italy). *Palaeogeogr.*
49
50
51 *Palaeoclimatol. Palaeoecol.*, **466**, 265–278.
52
53
54
55
56 CATTANEO, A., CORREGGIARI, A., LANGONE, L. AND TRINCARDI, F., 2003. The late-
57
58 Holocene Gargano subaqueous delta, Adriatic shelf: sediment pathways and supply fluctuations.
59
60 *Mar. Geol.*, **193**, 61–91.

- 1
2
3
4
5 CORREGGIARI, A., CATTANEO, A., TRINCARDI, F., 2005a. Depositional patterns in the Late-
6 Holocene Po delta system. In: *River Deltas—Concepts, Models and Examples* (Eds. J.P.
7 Bhattacharya and L. Giosan), *SEPM Spec. Publ.*, **83**, 365–392.
8
9
10
11
12
13
14 CORREGGIARI, A., CATTANEO, A., TRINCARDI, F., 2005b. The modern Po Delta system:
15 lobe switching and asymmetric prodelta growth. *Mar. Geol.*, **222**, 49–74.
16
17
18
19
20
21 CURZI, P.V., DINELLI, E., RICCI LUCCHI, M., VAIANI, S.C., 2006. Palaeoenvironmental
22 control on sediment composition and provenance in the late Quaternary deltaic successions: a case
23 study from the Po delta area (Northern Italy). *Geol. J.*, **41**, 591–612.
24
25
26
27
28
29
30 ENGE, H.D., HOWELL, J.A., BUCKLEY, S.J., 2010. The geometry and internal architecture of
31 stream mouth bars in the Panther Tongue and the Ferron Sandstone Members, Utah, U.S.A. *J.*
32 *Sedim. Res.*, **80**, 1018–1031.
33
34
35
36
37
38
39
40 GREGGIO, N., GIAMBASTIANI, B.M.S., CAMPO, B., DINELLI, E., AMOROSI, A., 2018.
41 Sediment composition, provenance and Holocene paleoenvironmental evolution of the Southern Po
42 River coastal plain (Italy). *Geol. J.*, **53**, 914–928.
43
44
45
46
47
48
49 JORISSEN, F.J., 1988. Benthic foraminifera from the Adriatic Sea; principles of phenotypic
50 variation. *Utrecht Micropaleontol. Bull.*, **37**, 1–176.
51
52
53
54
55
56 LAZAR, O.R., BOHACS, K.M., MACQUAKER, J.H.S., SCHIEBER, J., DEMKO, T.M., 2015.
57 Capturing key attributes of fine-grained sedimentary rocks in outcrops, cores and thin sections—
58 nomenclature and description guidelines. *J. Sed. Res.*, **85**, 230–246.
59
60

1
2
3
4
5 MACQUAKER, J.H.S., BENTLEY, S.J., BOHACS, K.M., 2010. Wave-enhanced sediment-gravity
6 flows and mud dispersal across continental shelves: reappraising sediment transport processes
7 operating in ancient mudstone successions. *Geology*, **38**, 947–950.
8
9
10
11
12

13
14 MADOF, A.S., HARRIS, A.D., CONNELL, S.D., 2016. Nearshore along-strike variability: Is the
15 concept of systems tract unhinged? *Geology*, **44**, 315–318.
16
17
18
19
20

21 MARCHESINI, L., AMOROSI, A., CIBIN, U., ZUFFA, G.G., SPADAFORA, E., PRETI, D.,
22 2000. Sand composition and sedimentary evolution of a Late Quaternary depositional sequence,
23 northwestern Adriatic Coast, Italy. *J. Sed. Res.*, **70**, 829–838.
24
25
26
27
28
29

30 MASELLI, V., TRINCARDI, F., 2013. Large-scale single incised valley from a small catchment
31 basin on the western Adriatic margin (central Mediterranean Sea). *Global Planet. Change*, **100**,
32 245–262.
33
34
35
36
37
38
39

40 OLARIU, C., STEEL, R.J., 2009. Influence of point-source sediment-supply on modern shelf-slope
41 morphology: implications for interpretation of ancient shelf margins. *Basin Res.*, **21**, 484–501.
42
43
44
45
46

47 PELLEGRINI, C., MASELLI, V., GAMBERI, F., ASIOLI, A., BOHACS, K.M., DREXLER,
48 T.M., TRINCARDI, F., 2017. How to make a 350-m-thick lowstand systems tract in 17,000 years:
49 The Late Pleistocene Po River (Italy) lowstand wedge. *Geology*, **45**, 327–330.
50
51
52
53
54
55

56 PELLEGRINI, C., ASIOLI, A., BOHACS, K.B., DREXLER, T.M., FELDMAN, H.R., SWEET,
57 M.L., MASELLI, V., ROVERE, M., GAMBERI, F., DALLA VALLE, G., TRINCARDI, F., 2018.
58
59
60

1
2
3 The late Pleistocene Po River lowstand wedge in the Adriatic Sea: Control on architecture
4 variability and sediment partitioning. *Mar. Petrol. Geol.*, **96**,16-50.
5
6
7
8
9

10 ROSSI, V., VAIANI, S.C., 2008. Benthic foraminiferal evidence of sediment supply changes and
11 fluvial drainage reorganization in Holocene deposits of the Po Delta. *Mar. Micropaleontol.*, **69**,
12 106–118.
13
14
15
16
17
18

19 TRINCARDI, F., CATTANEO, A., ASIOLI, A., CORREGGIARI, A. AND LANGONE, L., 1996.
20 Stratigraphy of the Late-Quaternary deposits in the central Adriatic basin and the record of short
21 term climatic events. *Mem. Istit. Ital. Idrobiol.*, **55**, 39–70.
22
23
24
25
26
27
28
29
30
31
32
33
34
35
36
37
38
39
40
41
42
43
44
45
46
47
48
49
50
51
52
53
54
55
56
57
58
59
60

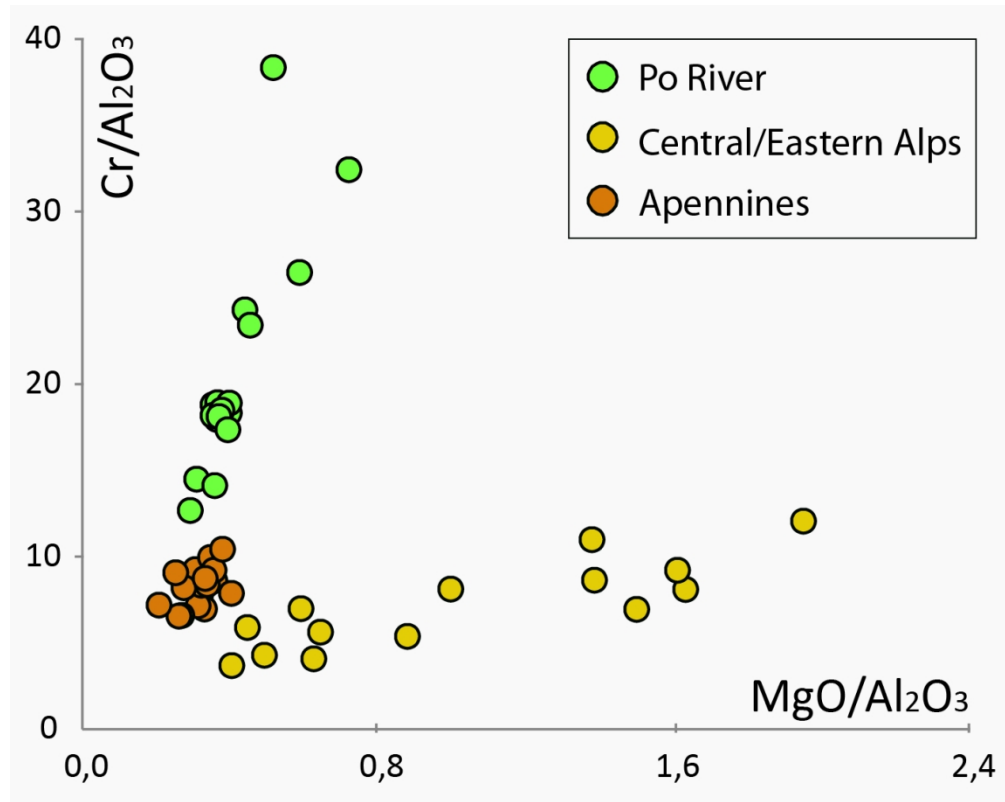


Fig. 2. Scatterplots of MgO/Al_2O_3 versus Cr/Al_2O_3 , showing contrasting sediment composition of modern Po River, and selected Alpine and Apennine rivers.

119x95mm (300 x 300 DPI)

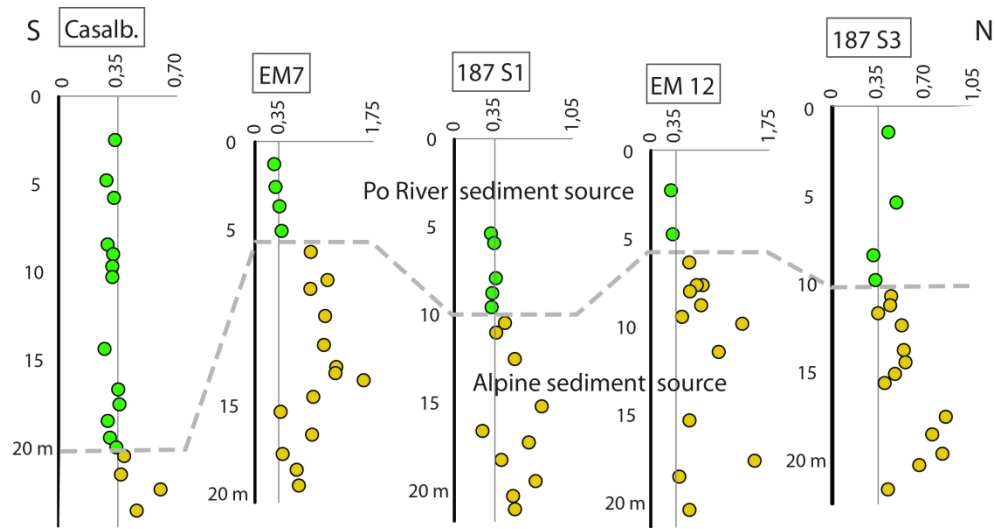


Fig. 3. Vertical profiles of MgO/Al_2O_3 in along-strike direction (Fig. 1B), showing the abrupt provenance shift from predominantly Alpine sediment sources to the Po River sediment supply (see

249x129mm (300 x 300 DPI)

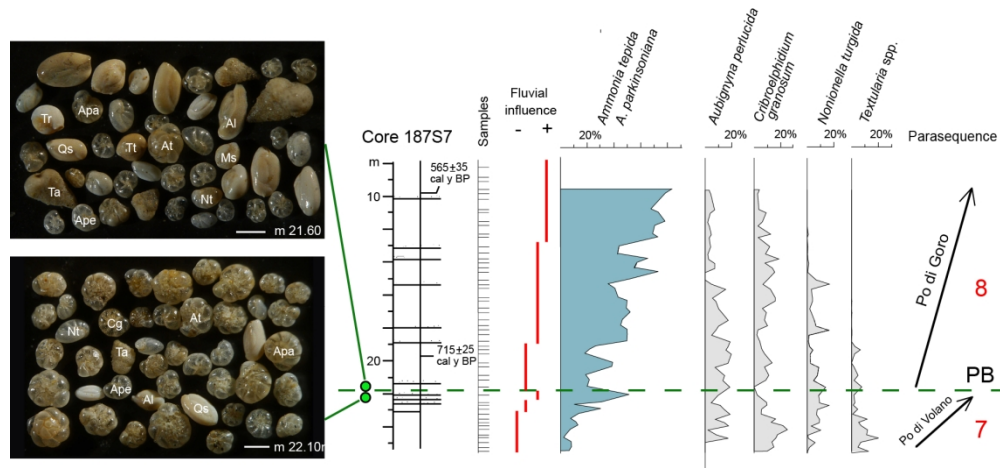


Fig. 4. Abrupt change in foraminiferal assemblage at the boundary (PB) between Po di Volano and Po di Goro delta lobes (= boundary between parasequences 7 and 8 in core 187-S7 - Figs. 1B and 5). Sample at 22.10 m depth is dominated by *Ammonia tepida* (At) and *A. parkinsoniana* (Apa), whereas sample at 21.60 m depth, just above PB, shows a significantly more diversified assemblage, involving *Aubignyna per lucida* (Ape), *Nonionella turgida* (Nt), *Textularia agglutinans* (Ta), *Criboelphidium granosum* (Cg), and miliolids (Al: *Adelosina longirostra*; Qs: *Quinqueloculina seminulum*; Ms: *Miliolinella subrotunda*; Tr: *Triloculina rotunda*; Tt: *T. trigonula*). Scale bar: 200 μ m.

162x75mm (300 x 300 DPI)

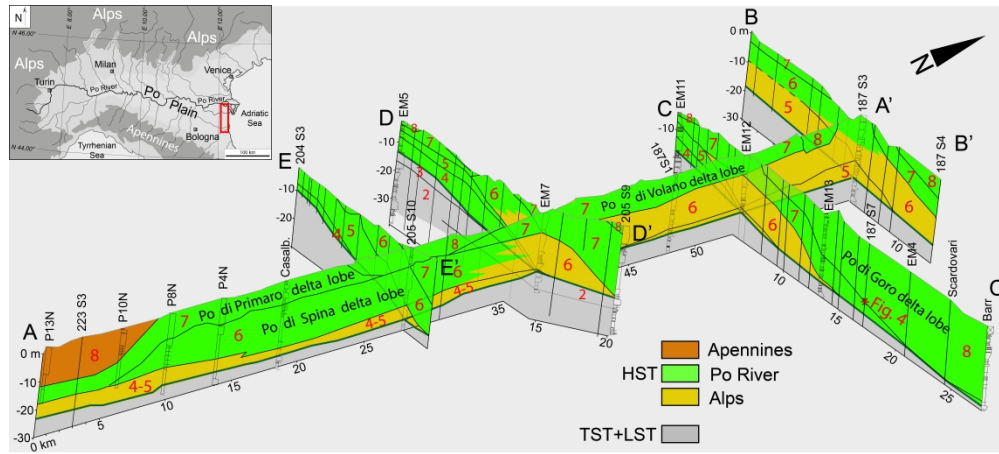


Fig. 5. Strike-oriented fence diagram of Figure 1B, which affords the visualization of the sediment-transport system as a function of parasequence architecture and of its evolution through time. The red asterisk shows the stratigraphic location of Figure 4. LST: lowstand systems tract, TST: transgressive systems tract, HST: highstand systems tract.

589x265mm (300 x 300 DPI)